PULTRUSION PROCESS SIMULATION – MODELLING OF THE INJECTION AND IMPREGNATION CHAMBER

Nik Poppe*[1], Michael Wilhelm[2] and Luise Kärger[1]

[1] Institute of Vehicle Systems Technology, Karlsruhe Institute of Technology, Karlsruhe, Germany
[2] Polymer Engineering, Fraunhofer Institute for Chemical Technology, Pfinztal, Germany
* Corresponding author (nik.poppe@kit.edu)

Keywords: Continuous fibres, Injection pultrusion, Moulding simulation, Finite volume method

ABSTRACT

This work describes the modelling of the injection and impregnation chamber in a closed pultrusion process. The described materials are a highly reactive thermoplastic resin and glass fibres. The developed method is based on continuous fluid dynamics and implemented in an open-source framework. By the application of a finite volume approach, insights are gained on injection of reactive thermoplastic resin, flow patterns of the resin and resin reaction, each as a function of time. The fibrous domain is modelled as porous medium. Pure resin areas are considered where the chamber geometry is not completely filled out by fibres. Flow patterns include flow recirculation and dead zones with stagnating flow that arise in the pure resin areas. Dead zones imply the build-up of deposits due to advancing resin reaction. Location of simulated deposits matches tendentially with experimental findings. The developed method also allows for qualitative simulation of the shutdown of pultrusion process.

1 INTRODUCTION

Pultrusion is a continuous and highly efficient production process for fibre reinforced profiles of constant cross section. Characteristics of the pultrusion process are high productivity, high degree of automation, high fibre volume fractions and remarkable flexural stiffness of profiles, making them suitable as structural components for various applications [1].

In pultrusion processes, continuous fibres provided on racks are impregnated with resin and pulled through a heated die. Within the die, the matrix reacts and the profiles obtain their cross-sectional shape. The die is followed by a free section for cooling of the profiles. At the end of the line, the profiles are cut to a specific length by a saw.

Depending on the manner of impregnation, two process configurations can be distinguished. The fibres can be impregnated in an open bath filled with resin. This is the conventional approach viable for unsaturated polyesters and other thermoset resin systems with high shelf life. On the other hand, impregnation can be conducted in a semi-closed chamber with resin injection, referred to as injection and impregnation chamber (ii-chamber). This type is called closed injection pultrusion. Some resin systems have to be processed in closed pultrusion such as highly reactive matrices, whose usage has increased rapidly over the last few years. Furthermore, stricter work safety regulations (e.g. reduction of styrene emissions) may require the use of ii-chambers as a nearly closed process configuration in near future. Figure 1 illustrates the process schematic of closed injection pultrusion.

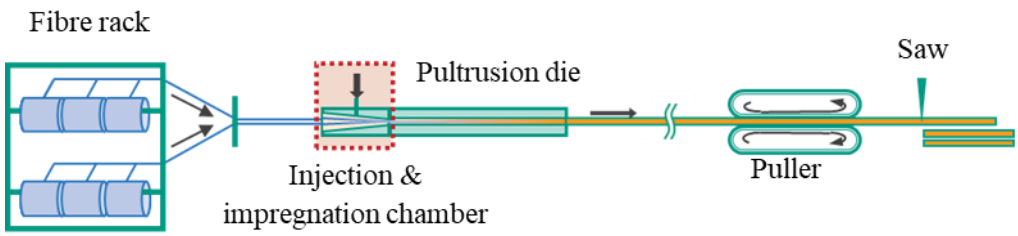

Figure 1: Process schematic of closed injection pultrusion.

By using reactive thermoplastic matrices such as nylon 6 and PMMA [2, 3], the process is nowadays named as in-situ pultrusion and is treated in this work. Although in in-situ pultrusion the polymerisation reaction is irreversible as with thermoset systems, thermoplastic profiles remain meltable, thus facilitating recycling and reducing the carbon footprint, while showing competitive mechanical properties [4]. Moreover, thermoplastic profiles enable for further processing and joining. Since some reactive thermoplastic matrices differ in viscosity by orders of magnitude from thermoset matrices, they require a new shape of ii-chambers. Non-reactive thermoplastics are also used to produce composite profiles. The process variants differ strongly from reactive pultrusion process in terms of the required machines and processing parameters [5].

Simulations with the finite volume method (FVM) can be used for design optimisation of ii-chambers by shedding light on flow phenomena occurring inside the closed box. Flow in the ii-chamber is governed by drag and pressure [6]. The specific orientation of drag direction and pressure gradient leads to an inhomogeneous velocity field with recirculating regions. A relevant aspect is the impregnation quality depending on profile cross section and ii-chamber design. Furthermore, simulations help to identify dead zones, i.e. regions with stagnating resin flow within the ii-chamber. Dead zones might be critical for long-term process stability since they increasingly induce deposits of partially cured resin at the chamber wall which can lead to instant process failure due to sudden detachment. The simulations presented in this work will enable virtual optimisation of ii-chamber design.

2 SIMULATION METHOD

Mathematical modelling of the pultrusion process has been reported in the literature since around 1980 [7]. The reported modelling approaches cover analytical models [6, 8] and numerical methods such as finite differences [9-11], finite elements [12-14] and also FVM [15, 16]. Literature on fluid dynamic modelling of in-situ pultrusion [17, 18] is very scarce, independent from the numerical method used. The main approach presented in literature for modelling of resin injection pultrusion in general, is based on commercial software with limited capabilities for method extensions [18-20]. The present work is based on simulations within the OpenFOAM® framework, an open-source software for continuous fluid dynamics (CFD). One key advantage in using open-source software is the possibility to examine and revise the complete code in detail, making the method transparent and highly flexible. These advantages of OpenFOAM® have been used for process simulation of various composite moulding processes before, like resin transfer moulding [21] and injection moulding [22], and shall now be utilised for pultrusion simulation.

The simulation approach applies the FVM. The simulated domain covers the volume of the ii-chamber cavity. The fibre bed is modelled as porous domain moving at a predefined haul-off speed. The resin flow is described by Darcy's law with the permeability depending on the local fibre volume fraction within the three-dimensional ii-chamber. Due to the specific chamber geometry, cf. Figure 2, the fibres do not fill the whole cavity but leave two free regions, one at the top, the other at the bottom, each next to the wall. Those regions are referred to as pure resin areas in the scope of this work and are described by the Navier-Stokes equation without the sink term related to porosity. A two-phase model is applied over the whole domain with the phases being resin and air. This enables prediction of impregnation quality. Complete impregnation of the fibres is vitally important for the mechanical properties of the profiles, so the ii-chamber design must enable the resin to permeate through the whole fibre stack. The two-phase model is implemented according to the volume of fluid method, where the phase volume fraction is given by a dimensionless variable for every part of the domain. In cells with both resin and air, viscosity and density are the average of both phases.

Caprolactam, the precursor of nylon 6, is exemplarily chosen as resin. Several factors have an impact on the resin properties, so three sub-models are included: for heat conduction, reaction kinetics and resin viscosity. The heat conduction model considers that the chamber can be differentially heated, and the fibres and resin both have their specific different temperature when entering the chamber. Heat release by the exothermic reaction is assumed to be negligible because the metal-composite interface is quite large compared to the cavity volume. Additionally, reaction enthalpy of caprolactam is small compared to thermoset materials [23]. Therefore, the heat conduction equation is implemented in its homogeneous formulation, i.e. without a source term. For reaction kinetics, the Kamal-Malkin model [24] is used. It

describes the reaction rate as a function of reaction degree and temperature. The Kamal-Malkin model was formulated for autocatalytic reactions with thermoset resin systems, but has been shown to describe the anionic polymerisation kinetics of nylon 6 correctly [25]. Resin viscosity is modelled as a function of temperature and reaction degree by the Castro-Macosko model [26]. For both the kinetic and the rheologic model, parameters have been estimated based on a single-run quasi-adiabatic measurement of a slower reacting formula. The coefficient of reaction rate has been extrapolated from that data in order to match approximately the experimental observations concerning the reaction duration.

The simulation model describes the injection and impregnation process over time. Unlike stationary simulations, this transient method calculates field results obeying the underlying laws of fluid dynamics for every single timestep. This allows representation of time-dependent phenomena such as filling of the ii-chamber at process start, build-up of deposits during the run or resin flow and curing at process shutdown. During the simulation, the time-step is adaptively chosen to comply the Courant condition in order to keep the simulation stable.

FVM, as the name implies, decomposes the domain into a number of finite volumes, and thus three-dimensional cells. Since a two-dimensional approach would reduce computational effort, the full-dimensional model is compared to simulation of a longitudinal section of the ii-chamber with a thickness of only one cell. This reduced model does not take into account the side walls and assumes perfect lateral homogeneity.

The examined chamber geometry is conically tapered with a narrower piece of constant cavity height attached to the broader opening, resulting in an abrupt increase of height where the conical part begins. That is where the pure resin areas are located (Figure 2). Given the low viscosity of molten caprolactam, a single injection point is chosen, positioned at the upper side of the chamber. The cavity volume is spatially discretised by 263.680 purely hexahedric cells. Refining the grid towards the walls proved to be necessary for correct modelling of boundary layers.

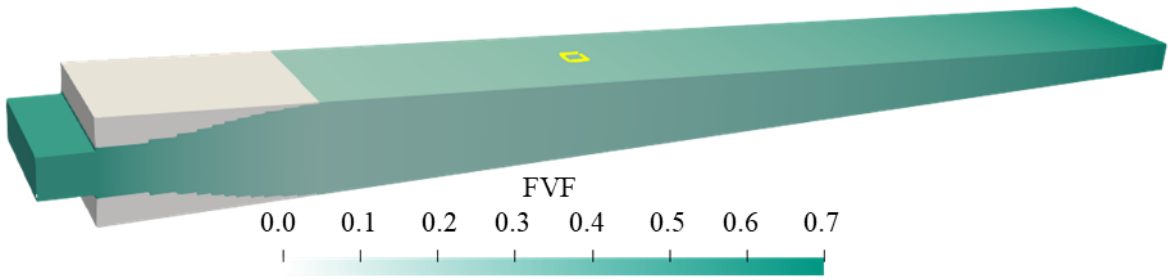

Figure 2: II-chamber geometry coloured by local fibre volume fraction. Fibres are pulled from left to right, resin is injected at the top wall (marked in yellow).

The system of equations needs boundary conditions for every field to ensure the uniqueness of the solution. Boundary conditions have been chosen to represent the process conditions as exactly as possible. Special care has been taken with the boundary condition for the field of reaction degree: At the walls of the pure resin area, a no-slip boundary condition is assumed for velocity. Hence, the resin at the walls remains at the same spot and reacts continuously without being transported. This is modelled by including the Kamal-Malkin model explicitly into the boundary condition.

Solution time is reduced by parallel execution of the software on a high-performance computer.

3 CONSISTENCY CHECKS

First verification of the simulation model is presented in the form of consistency checks. Therefore, the 2D case has been simulated with an additional injection port opposite the other, forming a symmetrical setup. The resulting flow field is well-balanced (Figure 3), even under the assumption of

gravitational force. Further consistency checks such as comparison of resin inflow, outflow and chamber filling rate have been conducted successfully.

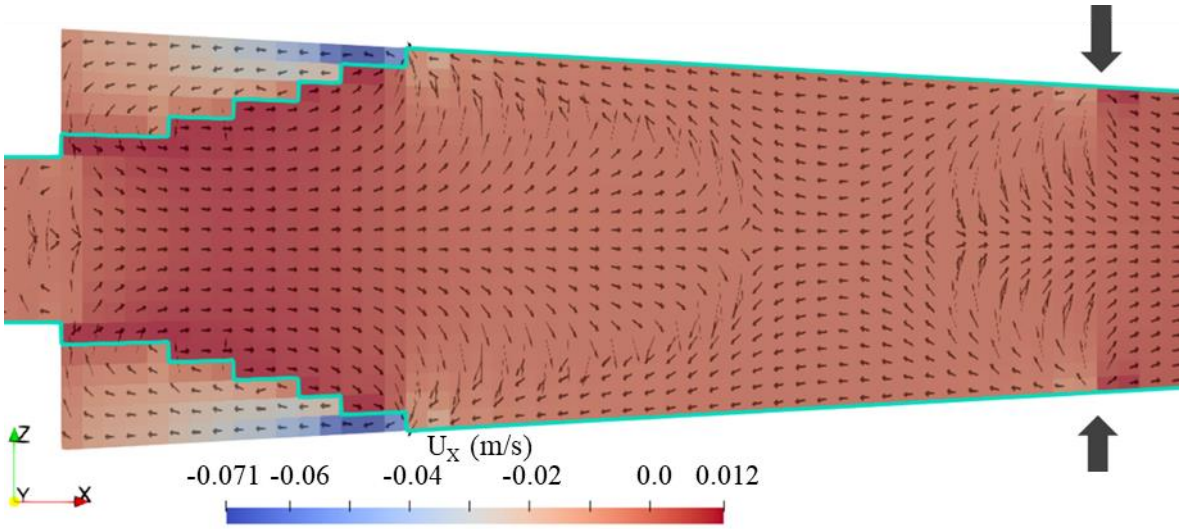

Figure 3: Detail of the flow field for the 2D configuration with symmetric injection ports marked by the two bold arrows. Fibres are pulled from left to right. The velocity vector field is represented by vector glyphs, the colour corresponds to the horizontal velocity component. The stepped green lines show the boundaries between fibre-filled zone and pure resin areas.

The 3D setup shows a vertical symmetry plane at its normal configuration with only one injection port. The results were not fully symmetric though (compare Figure 5). This is presumably related to numerical effects and has not been examined further yet.

4 RESULTS

Simulations show the flow pattern of resin within the ii-chamber. Concerning resin deposits in the ii-chamber, the trend of 3D simulation outcomes matches with experimental results. The simplified 2D model is not able to reproduce dead zones, let alone deposits during resin injection. This indicates that the underlying assumption of lateral homogeneity is not suitable for deposit prediction. The ii-chamber sidewalls represent a major difference between 3D and 2D model as they favour the formation of deposits due to the larger contact area. However, 2D simulation of the shutdown of the process can efficiently show how the reaction of semi-cured deposits goes on after injection is stopped.

4.1 Flow pattern

The closed ii-chamber entails that the fluid flow cannot be observed in the pultrusion process. The presented model, however, enables the detailed view on the 3D flow field. As shown in Figure 4, the flow pattern has complex shape even if only the flow field along the symmetry plane is considered. Due to drag, the main flow direction is the pulling direction of the fibres. Behind the injection point, this is the only flow direction. From the injection point, the resin goes into all directions, i.e. there is a backflow region from the injection point towards the inlet. Backflow is driven by the pressure gradient due to the tapered chamber geometry [6, 8, 20]. As it comes to the pure resin areas, there are two closed loops where the resin is circulating and reacting gradually, forming the deposits.

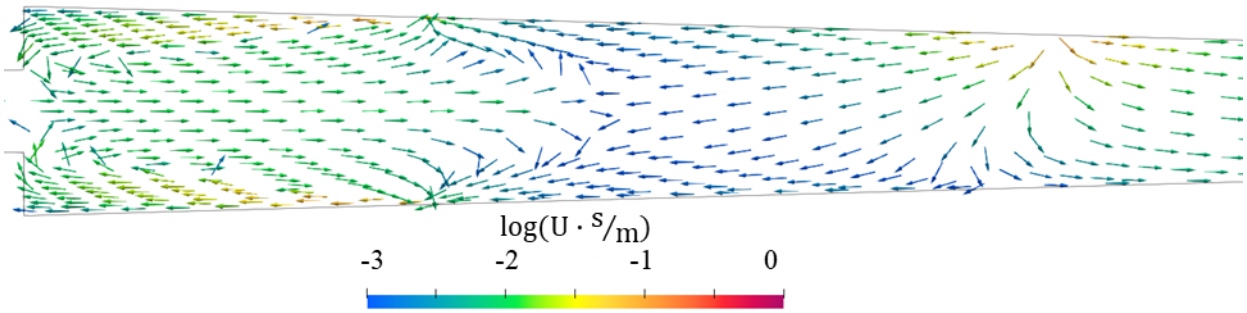

Figure 4: Detail of flow pattern after 20 s. The injection is located top right, fibres are pulled from left to right. Vector glyphs show the direction of fluid flow at their starting point. The vector length does not depend on resin speed, only their colour does. Resin speed ranges on several orders of magnitude, therefore the colour bar is logarithmically scaled. Vectors pointing out of the chamber only mean that the resin at the centers of the wall-adjacent cells flows towards the wall.

4.2 Resin deposits

The resin deposits observed in 3D simulation are located at the upper and lower wall in the pure resin areas. The deposits grow continuously starting from the walls, especially the edges. The lower deposit grows earlier than the upper deposit. This is mainly attributed to the location of the injection point at the upper wall. After a simulated time of 390 s, pure resin areas are almost completely filled with deposit showing a reaction degree of at least 60%. Spatial distribution shows qualitative agreement with experimental findings, however simulated deposits cover a smaller surface. Figure 5 shows simulated deposits as observed after 390 s and experimental deposits after 1 hour process time. The large difference on the time scale indicates the need for precise characterisation of the used resin system in order to find accurate parameter for Kamal-Malkin and Castro-Macosko model.

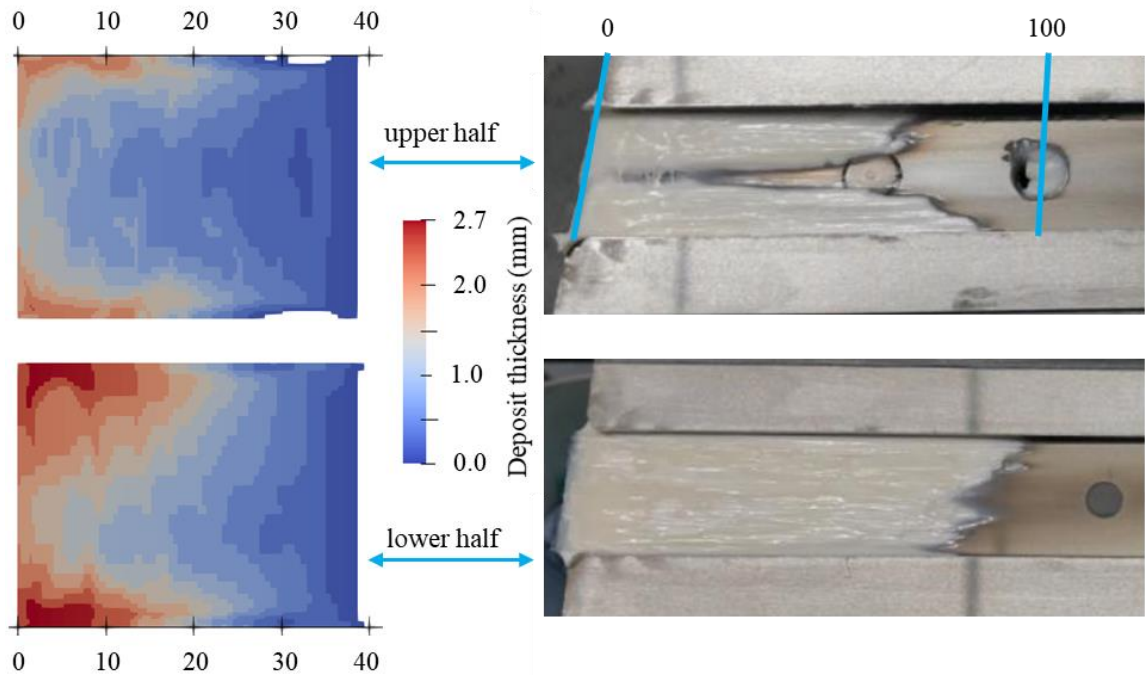

Figure 5: Comparison of simulated (left) and experimental (right) deposits for upper and lower half of the ii-chamber. Deposits depicted on the left are all cells with degree of reaction larger than 60%. Colours refer to deposit thickness.

4.3 2D model of the shutdown process

The 2D model was not able to reproduce resting resin. A circulating region including the pure resin areas is observed where the reaction is proceeding, but after some time the recirculation shows an overflow (drop of semi-cured resin travelling towards the outlet). So in that model, no amount of resin is restricted to a certain region as long as the injection is ongoing. However, when injection is stopped in 2D simulation and the chamber fills more and more with air, some resin stays in the pure resin areas and shows ongoing reaction. This prediction is relevant to method development for resin deposit assessment. Deposits should be assessed for a validation of the 3D simulation results (compare Figure 5). Due to the closed chamber, this can only be done after shutdown of the process. Shutdown itself takes some time, and during this time, deposits can react or grow further or even start to form, as in the 2D model. Figure 6 shows the field of reaction degree before and after shutdown in the 2D model. This result indicates that care should be taken when measuring deposit degree of cure.

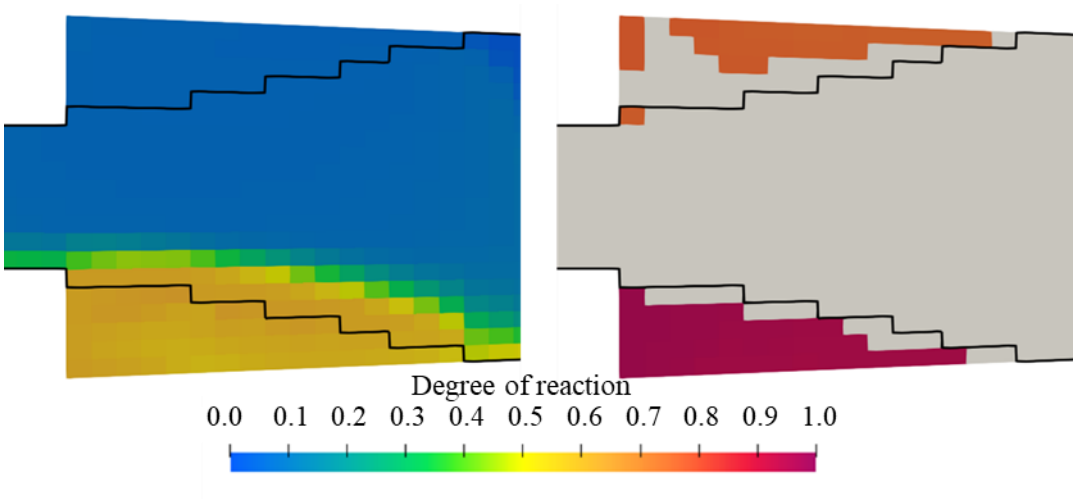

Figure 6: 2D-Simulation of shutdown process: degree of reaction before stopping the injection (left) and 95 s later (right). Cells without resin are coloured in grey. Boundaries of fibre-filled region are marked by black lines.

5 CONCLUSIONS

This article presents a method for three-dimensional simulation of in-situ pultrusion based on an open-source FVM framework. It is focused on the ii-chamber. Apart from the fundamental quantities pressure and fluid velocity, the model includes temperature, cure, cure-dependent viscosity, fiber volume content and an additional air phase. The method discloses the flow pattern inside the ii-chamber including backflow, recirculation and stagnating flow. It allows the prediction of progressing resin reaction in the dead zones, inducing the build-up of resin deposits. Simulated deposits show qualitative agreement to experimental findings. Additionally, simulation of the shutdown process shows how deposits can be affected before the chamber is opened.

In order to calibrate the models presented in this work and obtain quantitative results, experimental characterisation of the materials needs to be performed. For definition of a viable processing window for a given profile cross section by means of simulations, impregnation of fibres in the ii-chamber has to be investigated further. Beyond the ii-chamber, modelling of the pultrusion die will enable prediction of polymerisation quality, warpage and further process-specific quantities.

ACKNOWLEDGEMENTS

This research on pultrusion simulation was funded by the Ministry of Economics, Labour and Tourism Baden-Württemberg ("CaproPULL" Grant No ibwip-BW1_0025). Modelling of material behaviour and process boundary conditions was also supported by the German Research Foundation in project KA 4224/9-1, No. 449100283.

REFERENCES

[1] A. Vedernikov, A. Safonov, F. Tucci, P. Carlone, I. Akhatov, Pultruded materials and structures: A review, *Journal of Composite Materials*, **54**(26), 2020, pp 4081-4117.

[2] R. Emmerich, M. Wilhelm, Investigations to the effect of preheating the resin on the pultrusion process, *Proceedings of ITHEC 2022, 6th International Conference & Exhibition on Thermoplastic Composites*, 2022, pp. 127-130.

[3] A. Zoller, P. Escalé, P. Gérard, Pultrusion of bendable continuous fibers reinforced composites with reactive acrylic thermoplastic ELIUM® resin, *Frontiers in Materials*, **6,** 2019, 290.

[4] M. Wilhelm, *In-situ pultrusion of nylon 6 based profiles – material properties and recycling*, Chicaco, USA, 2023.

[5] K. Minchenkov, A. Vedernikov, A. Safonov, I. Akhatov, Thermoplastic pultrusion: a review, *Polymers*, **13**(2), 2021, 180.

[6] Z. Ding, S. Li, H Yang, H. Engelen, P.M. Puckett, Numerical and experimental analysis of resin flow and cure in resin injection pultrusion (RIP), *Polymer Composites*, **21**(5), 2000, pp. 762-778.

[7] H.L. Price, *Curing and flow of the thermosetting resins for composite materials pultrusion*, Dissertation, Old Dominion University, Norfolk, 1979 (DOI: 10.25777/p6ct-3a23).

[8] D.-H. Kim, P.-G Han, G.-H. Jin, W.-I. Lee, A model for thermosetting composite pultrusion process, *Journal of Composite Materials*, **31**(20), 1997, pp. 2105-2122.

[9] R. Gorthala, J.A. Roux and J.G. Vaughan, Resin flow, cure and heat transfer analysis for pultrusion process, *Journal of Composite Materials*, **28**, 1994, 486.

[10] K.S. Raper, J.A. Roux, T.A. McCarty and J.G. Vaughan, Investigation of the pressure behavior in a pultrusion die for graphite/epoxy composites, *Composites Part A: Applied Science and Manufacturing*, **30**(9), 1999, pp. 1123-1132.

[11] I. Baran, *Modelling the pultrusion process of off shore wind turbine blades*, Dissertation, Technical University of Denmark, Lyngby, 2014.

[12] S.C. Joshi, Y.C. Lam, Three-dimensional finite-element/nodal-control-volume simulation of the pultrusion process with temperature-dependent material properties including resin shrinkage, *Composites Science and Technology*, **61**, 2001, pp. 1539-1547.

[13] M.M. Shokrieh, A.M. Aghdami, A dynamic transient model to simulate the time dependent pultrusion process of glass/polyester composites, *Applied Composite Materials*, **18**, 2011, pp. 585-601

[14] A. Vedernikov, A. Safonov, F. Tucci, P. Carlone, I. Akhatov, Modeling Spring-in of L-shaped structural profiles pultruded at different pulling speeds, *Polymers*, **13**, 2021, 2748.

[15] E. Barkanov, P. Akishin, N.L. Miazza, S. Galvez, ANSYS based algorithms for a simulation of pultrusion process, *Mechanics of Materials and Structures*, **24**(5), 2017, pp. 377-384.

[16] R. de Cassia Costa Dias, M.L. Costa, L. de Sousa Santos, R. Schledjewski, Kinetic parameter estimation and simulation of pultrusion process of an epoxy-glass fiber system, *Thermochimica Acta*, **690**, 2020, 178636.

[17] A. Celik, C. Bonten, Three-dimensional modeling of the thermoplastic PA6 in-situ-pultrusion, *26. Stuttgarter Kunststoffkolloquium*, lecture series 2, 2019, pp. 141-147.

[18] X. Ding, Q. He, Q. Yang, S. Wang, K. Chen, Numerical simulation of impregnation process of reactive injection pultrusion for glass fiber/PA6 composites, *Polymers*, **14**(4), 2022, 666.

[19] X.-L. Liu, A finite element/nodal volume technique for flow simulation of injection pultrusion, *Composites Part A: Applied Science and Manufacturing*, **34**, 2003, pp. 649-661.

[20] R. Menezes Bezerra, *Modelling and simulation of the closed injection pultrusion process*, Dissertation, Karlsruhe Institute of Technology (KIT), Karlsruhe, 2017 (doi: 10.5445/IR/1000079057).

[21] J. Seuffert, L. Kärger, F. Henning, Simulating mold filling in Compression Resin Transfer Molding (CRTM) using a three-dimensional finite-volume formulation, *Journal of Composites Science*, **2**(2), 2018, 23.

[22] F. Wittemann, R. Maertens, L. Kärger, F. Henning, Injection molding simulation of short fiber reinforced thermosets with anisotropic and non-Newtonian flow behavior, *Composites Part A*: *Applied Science and Manufacturing*, **124**, 2019, 105476.

[23] R.S. Davé, R.L. Kruse, L.R. Stebbins, K. Udipi, Polyamides from lactams via anionic ring-opening polymerization: 2. Kinetics. *Polymer*, **38**(4), 1997, pp. 939-947.

[24] M. Kamal, S. Sourour, Kinetics and thermal characterization of thermoset cure, *Polymer Engineering and Science*, **13**, 1973, pp. 59-64.

[25] J.J.E. Teuwen, A.A. van Geenen, H.E.N. Bersee, Novel reaction kinetic model for anionic polyamide-6, *Macromolecular Materials and Engineering*, **298**, 2013, pp. 163-173.

[26] J.M. Castro, C.W. Macosko, Studies of mold filling and curing in the reaction injection molding process. *American Institute of Chemical Engineers Journals*, **28**(2), 1982, pp. 250-260.